KSME Journal, Vol. 10, No. 4, pp. 435~442, 1996



# Thermal Shock/Fatigue Evaluation of FGM by AE Technique

**Jun-Hee Song*, Jae-Kyoo Lim** and H. Takahashi*****

*(Received March 5, 1996)*

This study has been carried out to analyze the thermal shock and fatigue characteristics of functionally gradient material(FGM). The thermal shock/fatigue tests were conducted at a specific temperature and fracture patterns were studied by SEM and AE. Also, thermal fracture behavior of plasma-sprayed FGM and conventional coating material(NFGM) was examined by acoustic emission technique under heating and cooling. Furnace cooling and air cooling tests were used to examine the effect of temperature change under various conditions. The conventional and FGM coatings were compared to heat-resistant property and fracture surface of these materials for each temperature history. Based on these results, some critical temperature at the onset of coating failure can be evaluated to characterize the thermal resistance of the materials. It turned out to be that FGM gives higher thermal property compared with NFGM by AE signal and fracture surface analysis.

**Key Words:** Functionally Gradient Material, Thermal Shock/Fatigue, Acoustic Emission, Thermal Barrier Coating

## 1. Introduction

Recently, the effort to increase the efficiency of gas turbine has been stimulated strongly because of the sharp increase in fuel cost and the requirments to improve the turbine performance. Thermal barrier coating(TBC) materials of advanced gas turbine blades are expected to enhance the thermal efficiency of the energy conversion system by primarily increasing the operating gas temperature. But, the main problem is how to develop durable thermal barrier coating materials to overcome severe condition. The conventional TBC is a two layer coating(NFGM), but this method presents a difficult problem that the coating spalls from substrate at the leading edge of gas turbine blade. So, a new coating technique of functionally gradient materials(FGMs) has been proposed to overcome this problem. The use of advanced TBCs has the potential to increase the engine efficiency by permitting increased gas inlet temperature at present metal temperature, or maintaining current gas inlet temperature and reducing coolant requirement and the efficiency drop associated with air-cooling (Wortman, et. al., 1990). Generally, FGMs can be utilized to extend life of gas turbine, but life prediction method of the coating has not been established yet (Gill, et. al., 1986 ; Miller, 1987). The typical fracture modes of TBC are oxidation, vertical crack, delamination and spallation due to cooling from the applied temperature (Miller, et. al., 1982 ; Wei, et. al., 1989).

In this study, TBC system with functionally graded layers was tested by cylindrical specimens in addition to conventional two layer coating system. The effects of cooling rate and holding time of thermal cycle on the thermal fracture were examined in order to identify most critical thermal load. Furthermore, acoustic emission(AE) monitoring was performed to detect the microfracture process in thermal cycles, and fracture

* Graduate school, Department of Precision Mechanical Engineering, Chonbuk National University, Chonju, Korea.

** Department of Mechanical Design, Chonbuk National University, Chonju, Korea.

*** Research Institute for Fracture Technology, Faculty of Engineering, Tohoku University, Sendai, Japan.

surfaces were examined by scanning electron microscopy(SEM).

## 2. Experiments

### 2.1 Test specimens

Specimens used in the thermal shock/fatigue test were the cylindrical FGM and the conventional ceramic/metal composites (NFGM). The cylindrical shape of specimens simulated the curvature of the leading edge of a gas turbine blade and its dimension and composition are shown in Fig. 1 and Table 1. As shown in the figure, the outer diameter of substrate was 8mm and its thickness was 2mm. In FGM, the graded layer of ceramics and bond coat, NiCrAlY was 0.75mm thick. NFGM consisted of the ceramic coating layer of 0.35mm thick and NiCrAlY of 0.15mm thick. The coating layers were plasma sprayed with NiCrAlY and $ZrO_2$-8%wt $Y_2O_3$ on stainless steel substrate (Watanabe, 1993).

### 2.2 Thermal shock/fatigue test

Schematic diagram of experimental set-up for furnace heating is shown in Fig. 2. The high temperature atmosphere was created with an electric furnace whose maximum temperature raised was 1200℃ and capacity was 4 kw. The heating process during testing was regulated by temperature controllers. The heating rate was in the range of 60℃/min, and the maximum temperature of 600~1000℃. Thermal shock/fatigue tests were conducted by the three thermal steps of heating, holding and cooling in each condition. Tests were performed to examine the following effects.

#### 2.2.1 The change of maximum heating temperature

In FGM and NFGM, they were heated from a room temperature to 800℃ and 1000℃ and then furnace-cooled after holding period of five minutes. Thermal fatigue conditions were tested in maximum temperatures of 700℃, 850℃ and 1000℃.

#### 2.2.2 The change of cooling rate

In some tests, specimens were subjected to air-cooling after the heating and cooling period of five minutes. In the case of FGM, the maximum temperature were 800℃, 900℃, 1000℃ and that of NFGM were 600℃, 700℃, 800℃, 900℃. In thermal fatigue tests, both FGM and NFGM were heated up to 750℃ and cooled

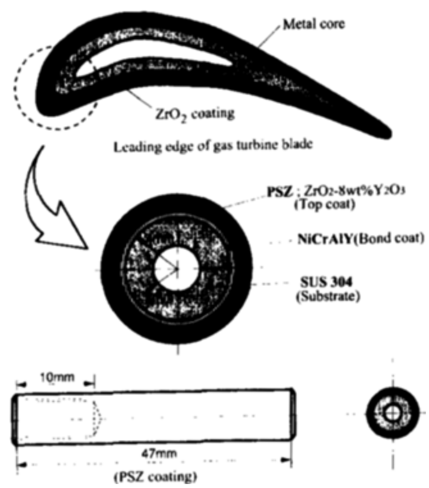


**Fig. 1** Cylindrical specimen for thermal shock test

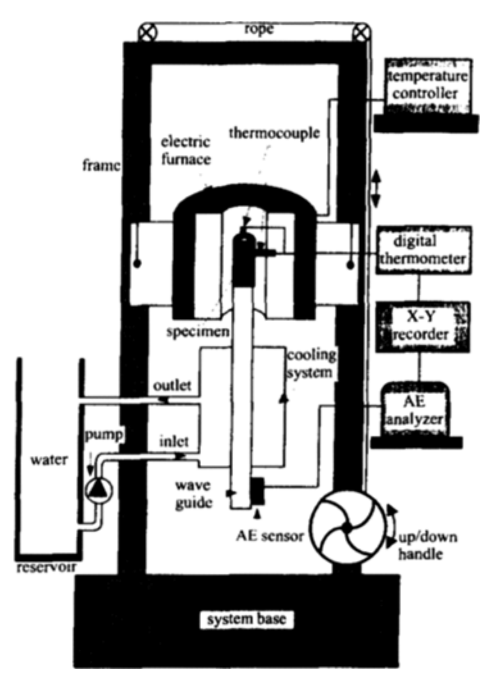


**Fig. 2** Thermal shock/fatigue testing system

rapidly in the air after holding for 5 minutes, and total cycles were 5 cycles.

#### 2.2.3 The change of holding time and cooling rate

Some specimens were exposed to 1 hour holding compared to the standard holding period of five minutes. NFGM and FGM were heated up to 800℃ and 1000℃, respectively and then they were subjected to air-cooling. In thermal fatigue tests, maximum temperature was 750℃ and total cycle was 6 cycles.

### 2.3 AE monitoring

AE monitoring was carried out using 8900 LOCAN AT ANALYZER made by Physical Acoustic Co.(PAC). The detected signals were amplified with a gain of 40dB in the preamplifier and filtered through 100 ~ 1200 kHz bandpass filter to reduced the background noise and then fed to AE analyzer. The AE electrical signals were amplified again with 40 dB in the main amplifier and analyzed using the A/D converter for signal processing. The threshold level for AE monitoring was set just above the background noises. Because of test conditions of high temperatures, AE sensor can't be directly attached to specimens. Thus a wave guide was inevitable, so an austenite stainless steel (STS304) rod with 450 mm in length and 10mm in diameter was used as the wave guide in this experiment.

Also, AE energy parameter is the measured area under the rectified signal envelop and it is responsive to both amplitude and duration of the event. AE energy is stored in 'dB'.

## 3. Test Results and Discussion

### 3.1 Thermal shock test

Test specimens of FGM and NFGM were analyzed by comparing their failure modes and AE behaviors, and then their cross-sections were observed by SEM. The valid analysis of the fracture mechanisms in the coatings interface is very important because it provides the basic data for structural integrity, material design and manufacturing.

#### 3.1.1 Standard heating-cooling cycle

This specimens were heated from a room temperature to the maximum temperature at the rate of about 60℃/min, held during the five minutes under isothermal condition and they were furnace-cooled. As a result, few AE energy below 300dB was shown in both NFGM and FGM. Also, in their SEM observation, microcrack were studded in the ceramic part but there have no such large crack as vertical crack or delamination. AE activity occurred mainly during the cooling step.

#### 3.1.2 Effect of cooling rate

This section describes the effects of the different temperature histories for both NFGM and FGM. NFGM specimen which has been coated by the conventional coating method was tested at the maximum temperature of 600℃, 700℃, 800℃ and 900℃, and FGM was tested at 800℃, 900℃ and 1000℃, respectively. The surface and the interior temperatures of the specimen were measured using the two thermocouples during the test.

There was relatively less emission. The AE energy was 80 dB under the conditions of 600℃ and 700℃. Fig. 3(a) shows the result for the NFGM specimen that was heated up to 800℃ and then cooled in the air after isothermal holding for 5 mins. The surface and the interior temperatures of the specimen were indicated by solid line and dashed line respectively in the figure. The total AE energy during the test was 770 dB and the maximum AE energy was 350dB at 160℃ of surface temperature and 210℃ of interior temperature, and it is noticeable that the emission occurred only during cooling. But, as shown in Fig. 3(b) of FGM, AE energy of below 40 dB was often detected during the test but the total AE energy was small as only 180 dB. That is, seeing that AE emission was small, it was shown that FGM air-cooled at 800℃ was scarcely affected by such thermal history. NFGM conditions up to 700℃ have few AE energy and didn't have any damages attributed to thermal history. On the other hand, AE energy was increased at above 800℃, so it can be inferred that the damages were progressed in respect that a few emission of above 300 dB were detected. Compared with furnace-cooling and air-cooling test in NFGM, AE energy was detected largely as cooling rate was rapid and the temperature of AE occurrence position was lower by 100℃ in air-cooling test. But, AE activity was not affected by cooling rate at 800℃ in FGM.

In the specimens of FGM heated at 800℃ and 900℃, few AE energy was shown emission of 30 to 40 dB below. Fig. 4 shows the temperature distribution against time variation and AE energy behavior of FGM at 1000℃. The temperatures of the surface and the interior were similar to the previous cases but AE energy behaviors were distributed differently. The total AE energy occurred was 445 dB and there was the highest emission of 360 dB at 480℃ of surface temperature and 580℃ of interior. It can be known that AE activity has no influence on cooling rate up to 900℃, but differed greatly at 1000℃. That is, there were scarecely damages of the coating interface up to 900℃, but if it had been subjected to the temperature of above 1000℃, the local fractures would be occurred. In the air-cooling thermal shock test, it can be shown that the initation temperature of the failure in NFGM and FGM was 800℃ and 1000℃, respectively.

### 3.1.3 Effect of holding time

This section examines the effects of the different isothermal holding time at the maximum temperatures for both NFGM and FGM. Specimen was heated at the rate of 60℃/min and extended isothermal holding time to 1 hr and then cooled in the air. Typically, the maximum temperature was 800℃ in NFGM and 1000 ℃ in FGM and these data were compared with the results of previous tests.

Figure 5(a) is the results that were obtained by heating up to the maximum temperature of 800℃ for NFGM. The total AE energy of 640 dB was detected mainly during the period of cooling. Although the similar temperature history was imposed in the test, more active emissions took place in the 1hr extended test of holding time, comparing with Fig. 3 of 5 mins holding. Fig. 5(b) shows the thermal history and AE energy distribution observed for the FGM which was subjected to 1 hr holding period at 1000℃ and then air-cooled. It is seen that the majority of the AE activity took place during the cooling step rather than the heating step. The comparison with the result shown in Fig. 4 for holding time of 5

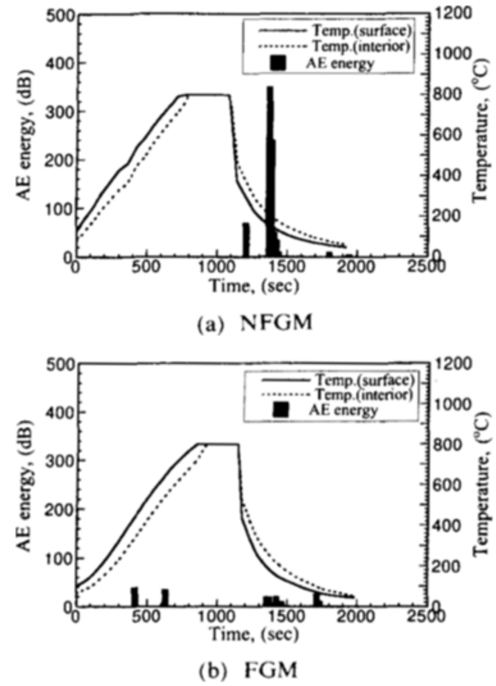


(a) NFGM

(b) FGM

**Fig. 3** AE behavior and temperature history by air-cooling in NFGM and FGM at 800℃

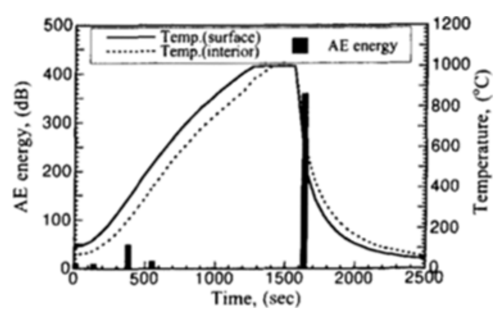


**Fig. 4** AE behavior and temperature history by air-cooling in FGM at 1000℃

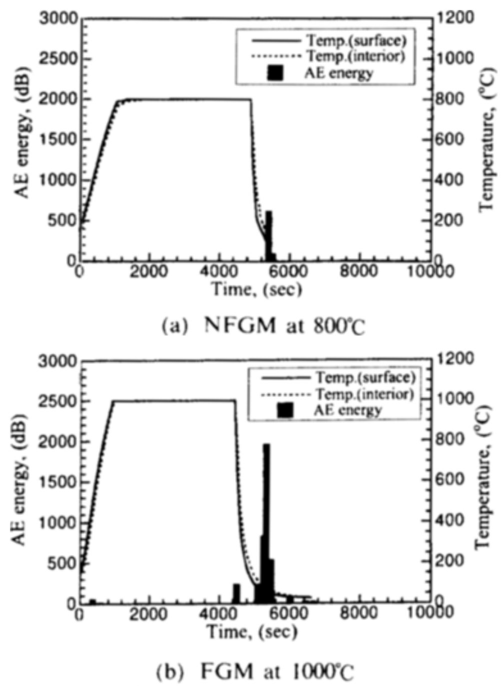


**Fig. 5** AE behavior and temperature history by air-cooling after 1 hr holding time

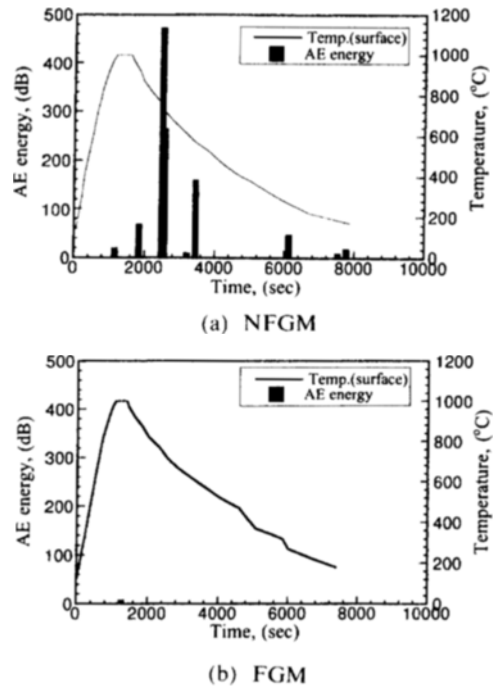


**Fig. 6** AE behavior and temperature history by furnace-cooling under thermal fatigue test in NFGM and FGM (4cycle)

mins. indicates that the AE activity for holding time of 1hr is ten times higher than that for 5mins and the extended holding time promotes the coating damage.

### 3.2 Thermal fatigue test

The method of thermal fatigue test was the same as that used in thermal shock test and the processes were cycled for several times.

#### 3.2.1 Standard heating-cooling cycle

NFGM and FGM were tested at the maximum temperature of 700℃, 850℃ and 1000℃ and the numbers of cycle were 4 cycles. Under the conditions of 700℃ and 850℃, only a few AE energy of 200dB below was occurred. Also, in cross section observation, there was microcrack and indistinct vertical crack but large failure didn't existed.

Figure 6(a) shows the temperature gradients with time and AE energy distribution in NFGM when the maximum temperature was 1000℃. The figure shows that the large AE energy of 470 dB was detected at the surface temperature of 700℃. That is, it can be judged that the material was damaged to the 4th thermal cycle at 1000℃. But, FGM under the same condition showed few emission in Fig. 6(b). Comparing with AE behaviors of NFGM and FGM, it can be clearly recognized that FGM is more superior to NFGM for the thermal fatigue resistance.

#### 3.2.2 Effect of cooling rate

This section describes the thermal fatigue effects of air-cooling. NFGM and FGM were conducted at the maximum temperature of 750℃ and the numbers of cycle were 5cycles. AE energy for all the cycles was extremly small, and below 250dB, so it can be shown that the thermal fatigue conditions of 5cycles couldn't affect to the specimens of NFGM and FGM.

#### 3.2.3 Effect of holding time

This section examines the thermal fatigue effect for the different holding time. The specimens of NFGM and FGM were heated up to 750℃ and then cooled in the air after isothermal holding for 1 hour. Total cycles were 6cycles. Figure 7(a) shows the temperature gradients and AE energy distribution in NFGM after 6cycle. The maximum AE energy was 320 dB during cooling. But, in Fig. 7(b) of FGM, small AE energy was detected as 220dB below. Also, it can be known that FGM is superior to NFGM for the thermal fatigue resistance.

In the thermal shock/thermal fatigue test, comparing with the temperature of surface and interior at the emission point of the maximum AE energy, the difference of these temperatures was about 100℃. But, in the case of 1hr-holding test AE energy emitted at about below 80 dB and the difference was also small. This was responsible for the fact that ceramic particles were subjected to the effect of creep by the 1hr-holding time under the high temperature.

### 3.3 Cross-section observation

Figure 8(a),(b) are the SEM photographes that were observed in a section of NFGM and FGM air-cooled after 5mins. isothermal holding at 800℃ and 1000℃, respectively. Microcracks were observed on the whole. In Fig. 8(a) of NFGM, delamination was formed, particularly in the cracks of long stripe shape at the interface regions of ceramics part and bond coat part. In Fig. 8(b) of FGM, vertical cracks were formed through the ceramics part and cracks were observed more than three positions on the section.

Figure 9(a),(b) are the SEM photographes that were observed in NFGM and FGM by standard heating-cooling cycle after 4cycles at 1000℃. In Fig. 9(a) of NFGM, delamination was formed in interface of ceramics and bond coat part. This length is about 1mm. But, in Fig. 9(b) of FGM, the vertical crack was formed througth the ceramics part. The level of crack is low and cracks were occurred in five places.

Figure 10(a),(b) are the SEM photographes that were observed in a section of FGM air-cooled after 1hr holding at 750℃ for thermal fatigue(6cycle). In Fig. 10(a) of NFGM, the

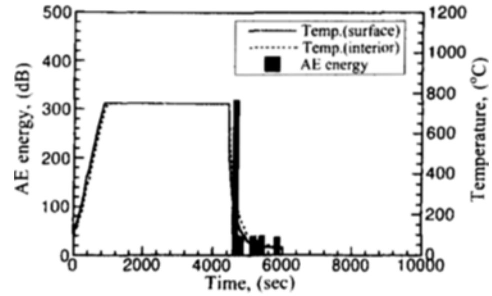


(a) NFGM

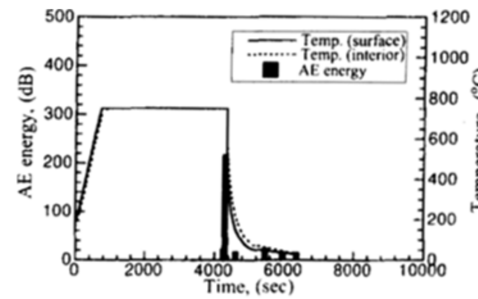


(b) FGM

**Fig. 7** AE behavior and temperature history by air-cooling under thermal fatigue test in NFGM and FGM (6cycle)

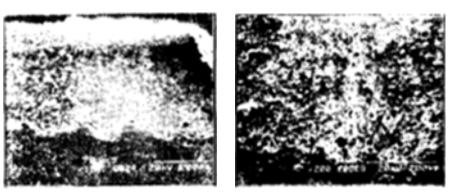

(a) NFGM at 800℃ (b) FGM at 1000℃

**Fig. 8** SEM photograph of air-cooling material by thermal shock test

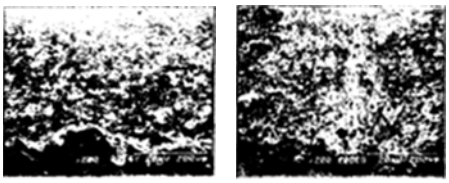

(a) NFGM (b) FGM at 1000℃

**Fig. 9** SEM photograph of furnace-cooling material by thermal fatigue test (4cycle) at 1000℃

**Table 1** Specification of coating in NFGM and FGM

| NFGM | | FGM | |
|---|---|---|---|
| Composition | Coating thickness(mm) | Composition | Coating thickness(mm) |
| PSZ 100% | 0.35 | PSZ 100% | 0.35 |
| | | PSZ 75%/NiCrAlY 25% | 0.1 |
| | | PSZ 50%/NiCrAlY 50% | 0.1 |
| NiCrAlY 100% | 0.15 | PSZ 25%/NiCrAlY 75% | 0.1 |
| | | NicrAlY 100% | 0.1 |
| Total thickness(mm) | 0.5 | Total thickness(mm) | 0.75 |

Substrate : SUS304 $\phi$ 8mm
$t$ 2mm

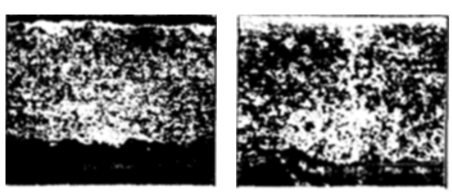

(a) NFGM (b) FGM

**Fig. 10** SEM photograph of air-cooling material after 1hr holding by thermal fatigue (6cycle) at 750℃

outstanding phenomenon is that delamination was formed through interface the ceramics and bond coat part. The length is about 0.5mm. In Fig. 10(b) of FGM, the vertical crack was formed insignificantly. But, the places occurred were many as seven positions.

In all SEM observation, these results are also in accord with the AE analysis and support effectively the method to detect propagation process of the crack by AE.

## 4. Conclusions

In this study, the fracture behaviors of FGM and NFGM were analyzed and evaluated by thermal shock and thermal fatigue tests under the high temperature atmosphere using AE. Also, the cross-section of each specimen was observed using SEM. The results obtained in this study can be summarized as belows :

(1) In the thermal shock test, the thermal effects depending on the cooling rate were different and AE energy was shown more emission in air-cooling test than furnace-cooling test. And AE behavior is large in 1hr-holding condition rather than 5minutes.

(2) In the thermal fatigue test, it could be known that AE behavior and fracture occurrence were different according to cooling condition and holding time, and that failures occurred at 1000℃ (4cycle) of furnace-cooling and 750℃ (6cycle) of 1hr holding time condition. Also, under the same condition, fracture level was more lower in FGM.

(3) At the SEM observations of all specimens, microcracks, vertical cracks and delaminations were observed and these results concurred with the results of AE analysis.

(4) In the thermal shock/thermal fatigue tests under the high temperature, many AE emissions and cracks occurred at 800℃ in NFGM and 1000℃ in FGM under air-cooling, so it could be found out the critical upper temperatures, and the majority of failures were propagated mostly during the cooling time.

## Acknowledgment

This study was been supported by the Korean Sience and Enginnering Foundation(KOSEF) under Grant No. 92-23-00-29. The authors would like to thank for the financial support of this work.

## References

Gill, B. J. and Tucker, R. C. Jr., 1986, "Plasma Spray Coating Processes," *Mater. Sci. Technol.*, 2, pp. 207~213.

Miller, R. A., 1987, "Current Status of Thermal Barrier Coatings," *Sur. & Coat. Technol.*, 30, pp. 1~11.

Miller, R. A. and Lowell, C. E., 1982, "Failure Mechanisms of Thermal Barrier Coatings Exposed to Elevated Temperatures," *Thin Solid Films*, Vol. 95, pp. 265~273.

Watanabe, R., 1993, "Functionally Gradient Material," *FGM Research Group and The Society of Non traditional Tech.*, pp. 306~310.

Wei, G. C. and Walsh, J., 1989, "Hot-Gas-Jet Method and Apparatus for Thermal-Shock Tetsing," *J. Am. Cera. Soc.*, Vol. 72, No. 7, pp. 1286~1289.

Wortman, D. J., Duderstadt, E. C. and Nelson, W. A., 1990, "Bond Coat Development for Thermal Barrier Coatings," *J. of Eng. for Gas Turb. and Pow.*, Vol. 112, pp. 527~530.